

Gas diffusion in nanoporous thin films

Leandro N. Acquaroli

Department of Engineering Physics, Ecole Polytechnique Montreal
P.O. Box 6079, Station Centre-Ville, Montreal (QC) H3C 3A7, Canada

July 25, 2019

We analyze the Fick's diffusion of a gas inside porous nanomaterials through the one-dimensional diffusion equation in nanopores for various cases of boundary conditions for homogeneous and non-homogeneous problems. We study the diffusion problems, starting without adsorption of the gas inside the pores, to more complex situations with surface adsorption in the pore walls and at the pore tips. Different methods of solution are reviewed depending on the problem, such as similarity transformation, Laplace transform, separation of variables, Danckwerts method and the Green's functions technique. The recovery step when the diffusion process stops and reached the steady-state is presented as well for the different problems.

I. Introduction

In the last decades, research on sensors fabricated with nanomaterials increased due to their broad range of applications from optoelectronics to sensors⁽¹⁻³⁾.

Porous silicon —PS— is a nanomaterial obtained by electrochemical anodization of crystalline silicon —c-Si— wafers in hydrofluoric acid —HF— solutions containing a surfactant such as ethanol —EtOH—. Under proper preparation conditions, a porous network grows inside the c-Si wafer with pores sizes varying from 2 nm up to 10 μm , and surface areas up to 800 $\text{m}^2 \text{g}^{-1}$. Due to these properties, its fast preparation and its diverse and tuneable optical, electrical and surface-chemical properties predestined PS for sensor and biosensor applications⁽⁴⁻¹⁰⁾.

We present an analysis of the different approaches to the one-dimensional diffusion equation, considering nanoscale mass transport inside a porous material. Consider a porous thin film on a substrate with an idealized cylindrical close-end pore —so that there is no net hydrodynamic flow into the pore, thus, neglecting advective transport— with length L_n and radius R_n —Fig. 1—. The transport always occurs in gas phase by neglecting Kelvin condensation in the nanopores. Adsorption and desorption time scales vary depending upon substrate surface and analyte species, but they typically fall in the range $\approx 10^{-6}$ s to 10^{-3} s, compared to the diffusion times in the 10^{-11} s. Considering the length and time scales above, the justifications for the use of the continuum assumption are not applicable. The requirement that the characteristic system length scale is large when compared to the characteristic molecular length scale is equivalent to the requirement that the Knudsen number, $K_n \equiv \mu\sqrt{RT/M}/(PR_n)$, be small. For instance, in PS nanopores, $K_n \approx 5$. Thus, it would appear that the continuum assumption should not be applied and that the governing equation for mass transport should be the more general Boltzmann transport equation. However, it has been demonstrated that a Fickian-like continuum model can still be used to describe mass transport in gasses at moderate Knudsen numbers provided the diffusion coefficient is appropriately modified to account for rarefaction effects⁽¹¹⁾.

We present the diffusion problems, from simple without adsorption to more complex situations with surface adsorption in the pore walls and at the pore tips. We review different methods of solution depending on the problem and the boundary conditions, such as similarity transformation, Laplace transform, separation

of variables, Danckwerts method and the Green's functions technique. We study as well the recovery step, when the diffusion process stops and reached the steady-state, for the different problems.

II. Diffusion problem at the nanoscale

A simplified version of the problem is reached assuming that the difference between the concentration at the pore wall and a cross-sectional area weighted average concentration are negligible. At least for short times, the fraction of active sites per unit area filled with the adsorbed species is negligible, and only adsorption —no desorption— occurs at an appreciable rate. Thus, removing the radial coordinate, the general dimensionless governing problem results as follow:

$$\text{(DE): } \partial_t c^* = \partial_{xx} c^* - \beta \alpha^2 c^*, \quad 0 < x^* < 1, \quad t^* > 0, \quad (\text{1a})$$

$$\text{(BC-1): } c^*(0, t^*) = 1, \quad t^* > 0, \quad (\text{1b})$$

$$\text{(BC-2): } \partial_x c^*(1, t^*) + \gamma \alpha^2 c^*(1, t^*) = 0, \quad t^* > 0, \quad (\text{1c})$$

$$\text{(IC): } c^*(x^*, 0) = 0, \quad 0 < x^* < 1, \quad (\text{1d})$$

where $c^*(x^*, t^*) = c(x, t)/c_0$ is the concentration normalized to the initial c_0 , $x^* = x/L_n$ is the dimensionless space coordinate, $t^* = t D_{Kn}/L_n^2$ is the dimensionless time, $D_{Kn} = R_n \sqrt{RT/M}$ is the Knudsen diffusion, with R is the universal gas constant, T is the temperature and M is the mole average molecular weight of the gas mixture. The parameter $\alpha = k_a L_n N / D_{Kn}$ where k_a is the rate coefficient for adsorption, and N the number of active sites per unit area of surface⁽¹¹⁾. The parameters β and γ serve to describe the general problem and will take values 0 or 1 depending on the different problems and boundary conditions considered.

III. Recovery process from diffusion

For sensing purposes, is interesting to determine the mathematical solution to the problem of diffusion, once the steady-state is reached and the point of diffusion is off. The steady-state is calculated taking the limit of the solutions of the diffusion problems discussed before when the time tends to infinity. Switching off the source of diffusion is done by setting the Dirichlet BC-1 (1b) to zero, giving the general problem for the normalized concentration

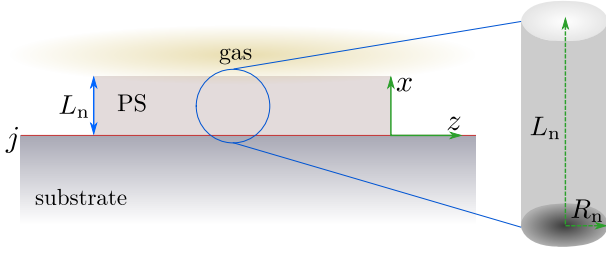


Fig. 1: Scheme of a nanoporous thin film surrounded by gas at the top and sitting on a solid substrate. The detail on the right shows an idealized cylindrical geometry used to analyze transient axisymmetric diffusion in a nanopore.

$u^*(x^*, t^*)$ as follow:

$$(DE): \quad \partial_t u^* = \partial_{xx} u^*, \quad (2a)$$

$$(BC-1): \quad u^*(0, t^*) = 0, \quad (2b)$$

$$(BC-2): \quad \partial_x u^*(1, t^*) = 0, \quad (2c)$$

$$(IC): \quad u^*(x^*, 0) = c^*(x^*, \infty). \quad (2d)$$

IV. Solutions to the diffusion problem without adsorption

We will tackle different approaches to solve the system (1) depending on the conditions established. First, we will consider the problem without adsorption, i.e., setting $\beta = \gamma = 0$ in (1) and solving the problem simplest diffusion equation with Dirichlet and Neumann boundary conditions using three different approaches.

IV.1. Similarity transformation

Similarity transformations to PDEs are solutions which relies on treating independent variables in groups rather than separately. Setting $\beta = \gamma = 0$ in problem (1) gives:

$$(DE): \quad \partial_t c^* = \partial_{xx} c^*, \quad (3a)$$

$$(BC-1): \quad c^*(0, t^*) = 1, \quad (3b)$$

$$(BC-2): \quad \partial_x c^*(1, t^*) = 0, \quad (3c)$$

$$(IC): \quad c^*(x^*, 0) = 0, \quad (3d)$$

We seek a solution of the form⁽¹²⁾

$$c^* = (t^*)^r g(\eta^*), \quad \eta^* = \frac{x^*}{\sqrt{t^*}}, \quad (4)$$

where r is chosen arbitrarily to satisfy the BCs. Then, we plug (4) into (3a):

$$\partial_t c^* = (t^*)^{r-1} r g - (t^*)^{r-1} \frac{\eta^* g'}{2}, \quad (5a)$$

$$\partial_{xx} c^* = (t^*)^{r-1} g''. \quad (5b)$$

We set $r = 1/2$ to satisfy the BCs in the final transformed ODE:

$$(DE): \quad g'' + \frac{\eta^*}{2} g' - \frac{1}{2} g = 0, \quad (6a)$$

$$(BC-1): \quad g(\eta^* \rightarrow 0) \rightarrow 1, \quad (6b)$$

$$(BC-2): \quad g'(\eta^* \rightarrow \infty) \rightarrow 0. \quad (6c)$$

Using the transformation $g(\eta^*) = \eta^* f(\eta^*)$ in (6a) gives the differential equation: $\eta^* f'' + [2 + (\eta^*)^2/2]f' = 0$. Solving for f and

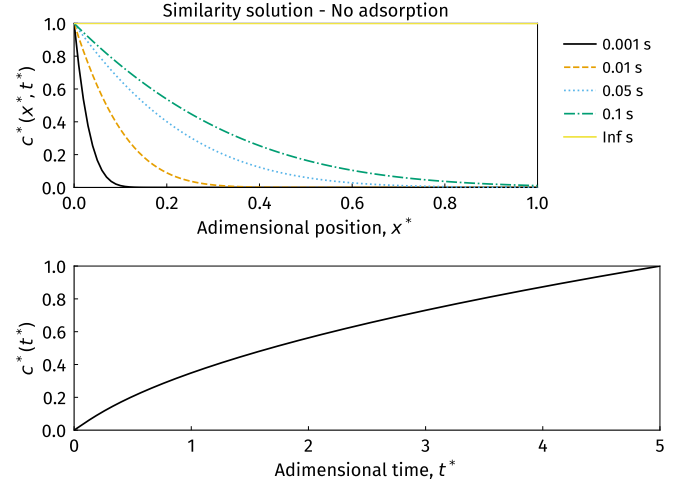


Fig. 2: Concentration profiles of the similarity solution: (top) Eq. (8) with legends indicating different t^* ; (bottom) Eq. (10).

applying the anti-transformation, we get:

$$g(\eta^*) = \frac{1}{2} \left[2 \exp(-(\eta^*)^2/4) - \sqrt{\pi} \eta^* + \eta^* \operatorname{erf}(\eta^*/2) \right]. \quad (7)$$

Thus, combining Eqs. (4) and (7), the solution of (3) results as follow:

$$c^*(x^*, t^*) = \sqrt{t^*} \exp\left(-\frac{x^*}{4t^*}\right) - \frac{\sqrt{\pi}}{2} x^* \operatorname{erfc}\left(\frac{x^*}{2\sqrt{t^*}}\right). \quad (8)$$

Integration of (8) over x^* yields the time solution of the concentration:

$$\begin{aligned} c^*(t^*) &= \int_0^1 c^*(x^*, t^*) dx^* \\ &= \frac{1}{2} \sqrt{t^*} \exp\left(-\frac{1}{4t^*}\right) + \frac{\sqrt{\pi}}{4} \left[(1 + 2t^*) \operatorname{erf}\left(\frac{1}{2\sqrt{t^*}}\right) - 1 \right]. \end{aligned} \quad (9)$$

$$(10)$$

Equation (8) shows a decay behavior which strongly depends on t^* , while the time profile of Eq. (10) builds up until it reaches the end of the pore, without clear saturation —Fig. 2—.

IV.2. Laplace transform

The method of Laplace transform is widely used in the solution of time-dependent diffusion problems because the partial derivative with respect to the time variable is removed from the differential equation of diffusion and replaced with a parameter, s , in the transformed field. Thus, this technique to solve PDEs is relatively straightforward, however, the inversion of the transformed solution generally is rather involved unless the inversion is available in the standard Laplace transform tables^(13,14). In fact, to simplify the inverse of the Laplace transform in our problem, we change the limits of the BCs, as if we flipped the thin film in the spatial coordinate. By setting $\beta = \gamma = 0$ in (1), we get:

$$(DE): \quad \partial_t c^* = \partial_{xx} c^*, \quad (11a)$$

$$(BC-1): \quad \partial_x c^*(0, t^*) = 0, \quad (11b)$$

$$(BC-2): \quad c^*(1, t^*) = 1, \quad (11c)$$

$$(IC): \quad c^*(x^*, 0) = 0, \quad (11d)$$

We start by taking the Laplace transform, \mathcal{L} , of each term of (11) as follow:

$$\mathcal{L}[\partial_{xx}c^*] = \hat{c}''(x^*, s), \quad (12a)$$

$$\mathcal{L}[\partial_t c^*] = s \hat{c}(x^*, s) - c^*(x^*, 0) = s \hat{c}(x^*, s), \quad (12b)$$

$$\mathcal{L}[\partial_x c^*(0, t^*)] = \mathcal{L}[0] = \hat{c}'(0, s) = 0, \quad (12c)$$

$$\mathcal{L}[c^*(1, t^*)] = \mathcal{L}[1] = \hat{c}(1, s) = \frac{1}{s}, \quad (12d)$$

where the variable $\hat{c} = \hat{c}(x^*, s)$ represents the concentration in the transformed field, where s is a parameter, not a variable. Then, the PDE of problem (11) is transformed into the following ODE:

$$(DE): \quad \hat{c}'' - s\hat{c} = 0, \quad (13a)$$

$$(BC-1): \quad \hat{c}'(0, s) = 0, \quad (13b)$$

$$(BC-2): \quad \hat{c}(1, s) = \frac{1}{s}, \quad (13c)$$

The general solution for problem (13) has the form⁽¹⁴⁾

$$\hat{c} = A_1 \cosh(x^* \sqrt{s}) + A_2 \sinh(x^* \sqrt{s}), \quad (14a)$$

$$\hat{c}' = A_1 \sqrt{s} \sinh(x^* \sqrt{s}) + A_2 \sqrt{s} \cosh(x^* \sqrt{s}). \quad (14b)$$

Applying the BCs to the solution (14), gives $A_1 = [s \cosh(\sqrt{s})]^{-1}$ and $A_2 = 0$. Plugging these constants into (14a), we get the solution in the transformed field:

$$\hat{c}(x^*, s) = \frac{\cosh(x^* \sqrt{s})}{s \cosh(\sqrt{s})}. \quad (15)$$

The inverse of the Laplace transform, \mathcal{L}^{-1} , of (15), is found in tables and gives the following solution to (11)⁽¹⁴⁾:

$$c^*(x^*, t^*) = \mathcal{L}^{-1}[\hat{c}(x^*, s)] \quad (16)$$

$$= 1 + 2 \sum_{n=1}^{\infty} \frac{(-1)^n}{\lambda_n} \cos(\lambda_n x^*) \exp(-\lambda_n^2 t^*). \quad (17)$$

where $\lambda_n = (n - 1/2)\pi$, $n \in \mathbb{Z}^+$. The time profile is —Eq. (9)—:

$$c^*(t^*) = 1 - 2 \sum_{n=1}^{\infty} \frac{1}{\lambda_n^2} \exp(-\lambda_n^2 t^*). \quad (18)$$

Solutions obtained with Laplace transform are plotted in Fig. 3.

IV.3. Separation of variables

The inverse of Laplace transform is useful when the anti-transformation is generally tabulated. Otherwise, it involves further complicated steps depending on the solution in the transformed field. The method of separation of variables presents as an alternative. To use this method, we split the problem (3) into an equilibrium steady-state part, $v(x^*)$, plus a non-equilibrium displacement part, $w(x^*, t^*)$ ⁽¹³⁾. By doing this, we send the non-homogeneity in BC-1 to the IC. Thus,

$$c^*(x^*, t^*) = v(x^*) + w(x^*, t^*), \quad (19)$$

The steady-state part problem is:

$$\left. \begin{array}{l} (DE): \quad v''(x^*) = 0 \\ (BC-1): \quad v(0) = 1 \\ (BC-2): \quad v'(1) = 0 \end{array} \right\} v(x^*) = 1. \quad (20)$$

The non-equilibrium problem is built from expression (19), $w^*(x^*, t^*) = c(x^*, t^*) - v(x^*)$, with homogenous BCs as follow:

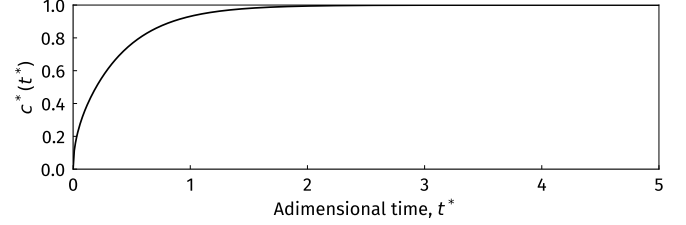
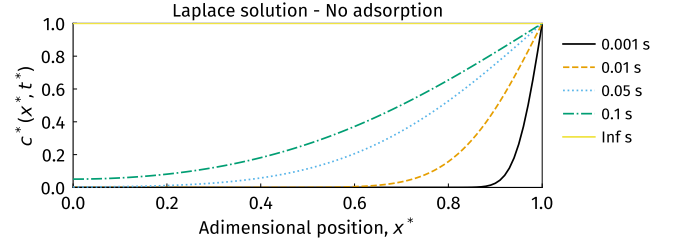


Fig. 3: Concentration profiles using the Laplace transform solution: (top) Eq. (17) with legends indicating different t^* ; (bottom) Eq. (18). Note the inversion of the boundary conditions.

$$(DE): \quad \partial_t w = \partial_{xx} w, \quad (21a)$$

$$(BC-1): \quad w(0, t^*) = 0, \quad (21b)$$

$$(BC-2): \quad \partial_x w(1, t^*) = 0, \quad (21c)$$

$$(IC): \quad w(x^*, 0) = c^*(x^*, 0) - v(x^*) = -v(x^*), \quad (21d)$$

where $c^*(x^*, 0) = 0$ in the IC results from (11d). Replacing $w(x^*, t^*) = p(x^*) q(t^*)$ in (21a) gives:

$$\frac{p''}{p} = \frac{q'}{q} = -\lambda^2, \quad (22)$$

where λ is an arbitrary separation constant. Last expression yields two ordinary differential equations for x^* and t^* . The x^* -dependent part satisfies the eigenvalue problem with two homogeneous boundary conditions as follow:

$$(DE): \quad p'' + \lambda^2 p = 0, \quad (23a)$$

$$(BC-1): \quad p(0) = 0, \quad (23b)$$

$$(BC-2): \quad p'(1) = 0. \quad (23c)$$

The general solution of (23) is

$$p(x^*) = A_1 \cos(\lambda x^*) + A_2 \sin(\lambda x^*), \quad (24a)$$

$$p'(x^*) = -A_1 \lambda \sin(\lambda x^*) + A_2 \lambda \cos(\lambda x^*). \quad (24b)$$

Placing the BCs we obtain the nontrivial solutions $A_1 = 0$ and $A_2 \cos(\lambda) = 0$. Since the cosine is a periodic function, the eigenvalue λ must satisfy the solution for every positive odd half-integer of π , hence, the eigenvalues are given by

$$\lambda_n = \left(n - \frac{1}{2}\right) \pi, \quad n \in \mathbb{Z}^+. \quad (25)$$

The eigenfunction corresponding to the eigenvalue λ_n is

$$p_n(x^*) = A_2 \sin(\lambda_n x^*). \quad (26)$$

The time-dependent ODE equation that results from (22)

$$q'(t^*) + \lambda^2 q(t^*) = 0 \quad (27)$$

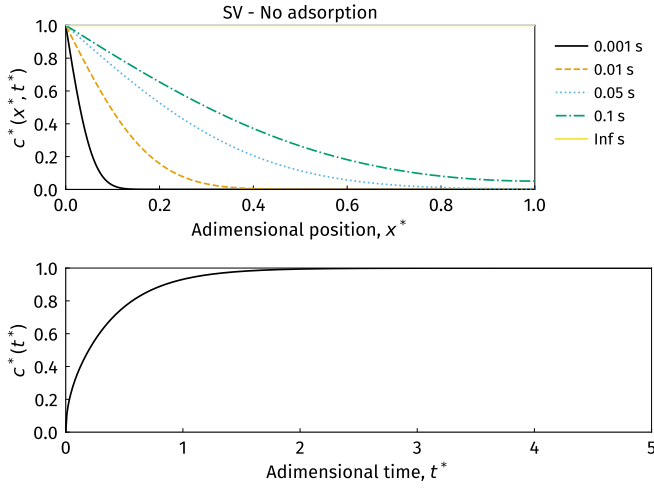


Fig. 4: Concentration profiles using the separation of variables solution: (top) Eq. (36) with legends indicating different t^* ; (bottom) Eq. (37).

has the following general solution:

$$q_n(t^*) = q(0) \exp(-\lambda_n^2 t^*). \quad (28)$$

Therefore, the product solution of (21) is

$$w_n(x^*, t^*) = B_n \sin(\lambda_n x^*) \exp(-\lambda_n^2 t^*). \quad (29)$$

where $B_n = A_2 q(0)$. The principle of superposition shows that w_n , with $n \in \mathbb{Z}^+$, are solutions of a linear homogeneous problem. It follows that any linear combination of these solutions is also a solution of the linear homogeneous equation (21). Thus, taking into account that B_n could be different for each solution, we have

$$w(x^*, t^*) = \sum_{n=1}^{\infty} B_n \sin(\lambda_n x^*) \exp(-\lambda_n^2 t^*). \quad (30)$$

The initial condition is satisfied if

$$w(x^*, 0) = -v(x^*) = \sum_{n=1}^{\infty} B_n \sin(\lambda_n x^*). \quad (31)$$

We first multiply both sides of (31) by $p_m(x^*)$ —for a given integer m of n —, and integrate over x^* :

$$-\int_0^1 v(x^*) \sin(\lambda_m x^*) dx^* = \sum_{n=1}^{\infty} B_n \int_0^1 \sin(\lambda_n x^*) \sin(\lambda_m x^*) dx^*. \quad (32)$$

The orthogonality property of the sine function implies that each term of the sum is zero whenever $n \neq m$, then, the only term that appears on the right-hand side occurs when m is replaced by n :

$$-\int_0^1 v(x^*) \sin(\lambda_n x^*) dx^* = B_n \int_0^1 \sin^2(\lambda_n x^*) dx^*. \quad (33)$$

Solving for B_n we obtain:

$$B_n = -\frac{\int_0^1 v(x^*) \sin(\lambda_n x^*) dx^*}{\int_0^1 \sin^2(\lambda_n x^*) dx^*} = -2 \int_0^1 v(x^*) \sin(\lambda_n x^*) dx^*. \quad (34)$$

Replacing $v(x^*) = 1$, results in

$$B_n = -2 \int_0^1 \sin(\lambda_n x^*) dx^* = -\frac{2}{\lambda_n}. \quad (35)$$

Combining Eqs. (19), (30) and (35), the final solution to the problem is:

$$c^*(x^*, t^*) = 1 - \sum_{n=1}^{\infty} \frac{2}{\lambda_n} \sin(\lambda_n x^*) \exp(-\lambda_n^2 t^*) \quad (36)$$

where the time-profile defined as

$$c^*(t^*) = 1 - \sum_{n=1}^{\infty} \frac{2}{\lambda_n^2} \exp(-\lambda_n^2 t^*). \quad (37)$$

and the eigenvalues given by (25). Plots of (36) and (37) are shown in Fig. 4.

V. Solutions to the diffusion problem with adsorption

Now we will consider two approaches to solve the system (1) with adsorption. There are solutions to this problem in literature, for $\beta = 1$ and $\gamma = 0$, giving rise to the surface adsorption effect inside the pores' walls, except at the bottom of the pore. We review this problem and also the solution for the Robin—mixed—boundary condition, $\gamma = 1$, when the adsorption at the pore-tip is considered.

V.1. Adsorption in the wall's surface of the pore

Setting $\beta = 1$ and $\gamma = 0$ in (1) becomes a reaction-diffusion problem with Dirichlet and Neumann boundary conditions as follow:

$$(DE): \quad \partial_t c^* = \partial_{xx} c^* - \alpha^2 c^*, \quad (38a)$$

$$(BC-1): \quad c^*(0, t^*) = 1, \quad (38b)$$

$$(BC-2): \quad \partial_x c^*(1, t^*) = 0, \quad (38c)$$

$$(IC): \quad c^*(x^*, 0) = 0. \quad (38d)$$

In the literature, exists solutions to this problem using eigenfunction expansion⁽¹¹⁾, superposition of solutions⁽¹⁵⁾ and Laplace transform⁽¹⁶⁾. Here, taking advantage to the constant nature of the BCs we solve this problem using the Danckwerts method⁽¹²⁾, which consists in solving the homogeneous DE, keeping the BCs and IC,

$$(DE): \quad \partial_t \hat{c} = \partial_{xx} \hat{c}, \quad (39a)$$

$$(BC-1): \quad \hat{c}(0, t^*) = 1, \quad (39b)$$

$$(BC-2): \quad \partial_x \hat{c}(1, t^*) = 0, \quad (39c)$$

$$(IC): \quad \hat{c}(x^*, 0) = 0. \quad (39d)$$

and then expressing the solution as follow:

$$c^*(x^*, t^*) = \alpha^2 \int_0^t \hat{c}(x^*, \tau) \exp(-\alpha^2 \tau) d\tau + \hat{c}(x^*, t^*) \exp(-\alpha^2 t^*). \quad (40)$$

Problem (39) is the same as (3), with solution given by Eq. (36). Thus, plugging this solution in (40), we get:

$$c^*(x^*, t^*) = 1 - \sum_{n=1}^{\infty} \frac{2}{\lambda_n} \sin(\lambda_n x^*) \left\{ \frac{\alpha^2 + \lambda_n^2 \exp[-(\alpha^2 + \lambda_n^2)t^*]}{(\alpha^2 + \lambda_n^2)} \right\},$$

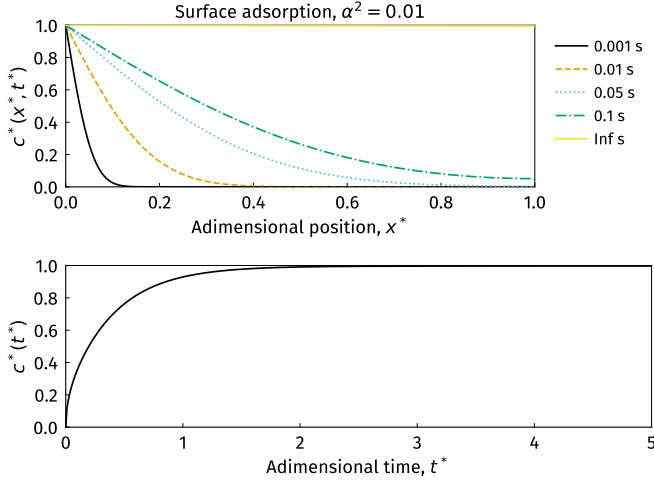


Fig. 5: Concentration profiles using the separation of variables solution: (top) Eq. (41) with legends indicating different t^* ; (bottom) Eq. (42). For all cases, $\alpha^2 = 0.01$.

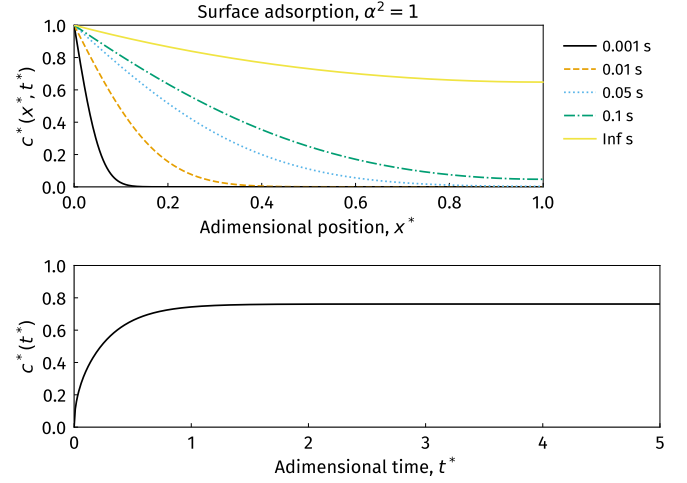


Fig. 6: Concentration profiles using the separation of variables solution: (top) Eq. (41) with legends indicating different t^* ; (bottom) Eq. (42). For all cases, $\alpha^2 = 1$.

(41)

with $\lambda_n = (n - 1/2)\pi$, $n \in \mathbb{Z}^+$. The time profile is given by:

$$c^*(t^*) = 1 - \sum_{n=1}^{\infty} \frac{2}{\lambda_n^2} \left\{ \frac{\alpha^2 + \lambda_n^2 \exp[-(\alpha^2 + \lambda_n^2)t^*]}{(\alpha^2 + \lambda_n^2)} \right\}. \quad (42)$$

Solutions of (41) are presented in Figs. 5 and 6 for different values of α^2 . Using Duhamel's theorem⁽¹⁴⁾ gives the same results.

V.2. Adsorption in the wall's surface and tip of the pore

Setting $\beta = 1$ and $\gamma = 1$ in (i) becomes the following reaction-diffusion problem with Dirichlet and Robin boundary conditions:

$$\text{(DE): } \partial_t c^* = \partial_{xx} c^* - \alpha^2 c^*, \quad (43a)$$

$$\text{(BC-1): } c^*(0, t^*) = 1, \quad (43b)$$

$$\text{(BC-2): } \partial_x c^*(1, t^*) + \alpha^2 c^*(1, t^*) = 0, \quad (43c)$$

$$\text{(IC): } c^*(x^*, 0) = 0. \quad (43d)$$

We define the transformation $c^* = \exp(-\alpha^2 t^*) \hat{c}$, and plug it into (43), which results as follow:

$$\text{(DE): } \partial_t \hat{c} = \partial_{xx} \hat{c}, \quad (44a)$$

$$\text{(BC-1): } \hat{c}(0, t^*) = \exp(\alpha^2 t^*) = f_1(t^*), \quad (44b)$$

$$\text{(BC-2): } \partial_x \hat{c}(1, t^*) + \alpha^2 \hat{c}(1, t^*) = 0 = f_2(t^*), \quad (44c)$$

$$\text{(IC): } \hat{c}(x^*, 0) = 0 = F(x^*). \quad (44d)$$

Notice that the transformation introduced not only removes the reaction term, but also replaces the Dirichlet BC-1 with a time-dependent condition, $f_1(t^*)$. For convenience, we wrote $f_2(t^*)$ as the BC-2, and $F(x^*)$ to the IC, although they are homogeneous. We solve problem (44) using the Green's function method⁽¹⁴⁾, where the solution expressed in terms of the Green's function, $G(x^*, t^* | x^\dagger, \tau)$,

is as follow:

$$\begin{aligned} \hat{c}(x^*, t^*) &= \int_0^1 G(x^*, t^* | x^\dagger, 0) F(x^\dagger) (x^\dagger)^m dx^\dagger \\ &+ \int_0^{t^*} \int_0^1 G(x^*, t^* | x^\dagger, \tau) g(x^\dagger, \tau) (x^\dagger)^m dx^\dagger d\tau \\ &+ \sum_{i=1}^N \int_0^{t^*} x_i^m G(x^*, t^* | x_i, \tau) f_i(\tau) d\tau \end{aligned} \quad (45)$$

where $(x^\dagger)^m$ is the Sturm-Liouville weight function with $m = 0$ for rectangular spatial coordinate, x_i is the i th boundary point of the total N boundary conditions prescribed, $g(x^*, t^*)$ is the generation term —eliminated by the transformation—, $F(x^*)$ is the initial condition, and $f_i(t^*)$ are the non-homogeneous boundary conditions functions. Notice that for a Dirichlet boundary condition, we should replace $G(x^*, t^* | x_i, \tau)$ by $\partial_{x^\dagger} G(x^*, t^* | x_i, \tau)$.

To find the Green's function that solves the problem, we first solve the associated homogeneous problem of (44):

$$\text{(DE): } \partial_t \psi = \partial_{xx} \psi, \quad (46a)$$

$$\text{(BC-1): } \psi(0, t^*) = 0, \quad (46b)$$

$$\text{(BC-2): } \partial_x \psi(1, t^*) + \alpha^2 \psi(1, t^*) = 0, \quad (46c)$$

$$\text{(IC): } \psi(x^*, 0) = F(x^*). \quad (46d)$$

Separation of variables, $\psi(x^*, t^*) = p(x^*)q(t^*)$, leads to the related boundary value problem of (46),

$$\text{(DE): } p'' + \lambda p = 0, \quad (47a)$$

$$\text{(BC-1): } p(0) = 0, \quad (47b)$$

$$\text{(BC-2): } p'(1) + \alpha^2 p(1) = 0, \quad (47c)$$

with eigenfunctions $p_n(x^*) = \sin(\lambda_n x^*)$ and the corresponding eigenvalues λ_n , defined as the roots of the transcendental equation, $\lambda_n \cot \lambda_n + \alpha^2 = 0$. When n tends to infinity, $\lambda_n \cot \lambda_n \sim (n - 1/2)\pi$. Thus, the eigenvalues express as $\lambda_n = (n - 1/2)\pi + \alpha^2$, $n \in \mathbb{Z}^+$. The difference comparing boundary value problems (47) with (23), lies in the eigenvalues due to the BC-2 conditions —Robin and Neumann— of the problem. The time-dependent solution is $q_n(t^*) = q(0) \exp(-\lambda_n^2 t^*)$, where the initial condition is

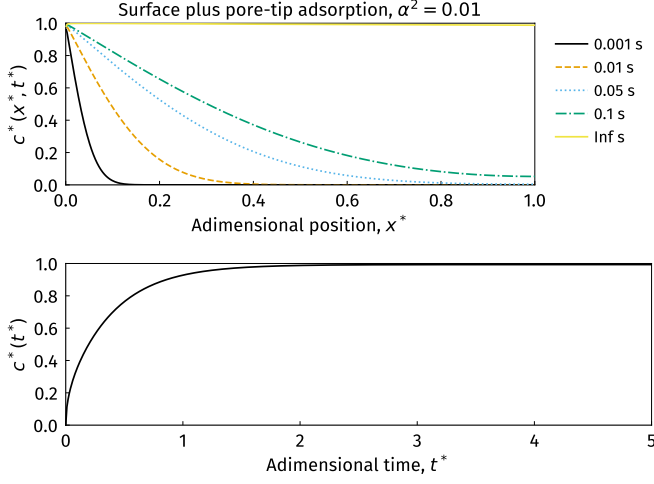


Fig. 7: Concentration profiles using the separation of variables solution: (top) Eq. (44) with legends indicating different t^* ; (bottom) Eq. (46). For all cases, $\alpha^2 = 0.01$.

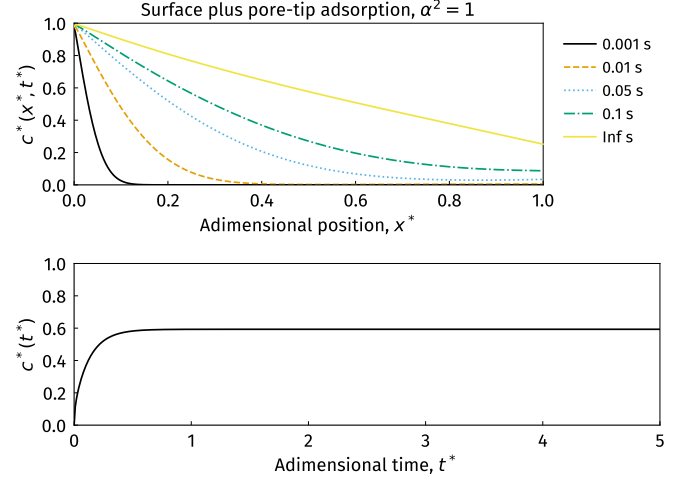


Fig. 8: Concentration profiles using the separation of variables solution: (top) Eq. (44) with legends indicating different t^* ; (bottom) Eq. (46). For all cases, $\alpha^2 = 1$.

obtained using the same procedure as before in Eqs. (31)-(34):

$$q(o) = 2 \int_0^1 p_n(x^\dagger) F(x^\dagger) dx^\dagger. \quad (48)$$

The solution of (46) is

$$\begin{aligned} \psi(x^*, t^*) &= \sum_{n=1}^{\infty} p_n(x^*) q_n(t^*) \\ &= \sum_{n=1}^{\infty} p_n(x^*) q(o) \exp(-\lambda_n^2 t^*) \\ &= \int_0^1 \left[\sum_{n=1}^{\infty} 2p_n(x^*) p_n(x^\dagger) \exp(-\lambda_n^2 t^*) \right] F(x^\dagger) dx^\dagger. \end{aligned} \quad (49)$$

Last equation establishes the solution to the associated homogeneous problem. Rearranging Eq. (49) expressed in the form

$$\psi(x^*, t^*) = \int_0^1 K(x^*, x^\dagger, t^*) F(x^\dagger) dx^\dagger. \quad (50)$$

implies that all the terms in the solution, except the initial condition function, are lumped into a single term $K(x^*, x^\dagger, t^*)$, called the kernel of the integration. Considering the Green's function approach for the solution of the same problem, the Green's function evaluated at $\tau = 0$ is equivalent to the kernel of integration: $G(x^*, t^* | x^\dagger, 0) \equiv K(x^*, x^\dagger, t^*)$. Hence, the kernel obtained by rearranging the homogeneous part of the transient problem into the form given by Eq. (50), represents the Green's function evaluated at $\tau = 0$. The full Green's function, $G(x^*, t^* | x^\dagger, \tau)$, is obtained replacing t by $t - \tau$ in $G(x^*, t^* | x^\dagger, 0)$ ⁽¹⁴⁾. Thus, the full Green's function determined from Eq. (49) is given by

$$\begin{aligned} G(x^*, t^* | x^\dagger, \tau) &= \sum_{n=1}^{\infty} 2p_n(x^*) p_n(x^\dagger) \exp[-\lambda_n^2 (t^* - \tau)] \\ &= \sum_{n=1}^{\infty} 2 \sin(\lambda_n x^*) \sin(\lambda_n x^\dagger) \exp[-\lambda_n^2 (t^* - \tau)] \end{aligned} \quad (51)$$

Now that we have calculated the Green's function, we proceed to solve problem (44), using (45), with $F(x^*) = 0$, $g(x^*, t^*) = 0$, and $f_2(t^*) = 0$ in the BC-2. Also, since the BC-1 is of the first type, we replace G by $\partial_{x^\dagger} G$:

$$\partial_{x^\dagger} G(x^*, t^* | x_i, \tau) = \sum_{n=1}^{\infty} 2\lambda_n \sin(\lambda_n x^*) \cos(\lambda_n x^\dagger) \exp[-\lambda_n^2 (t^* - \tau)]. \quad (52)$$

Then, Eq. (45) reduces to the following:

$$\hat{c}(x^*, t^*) = \sum_{n=1}^{\infty} 2\lambda_n \sin(\lambda_n x^*) \left[\frac{\exp(\alpha^2 t^*) - \exp(-\lambda_n^2 t^*)}{(\alpha^2 + \lambda_n^2)} \right]. \quad (53)$$

The final solution to problem (43) is recovered taking the anti-transformation, $c^* = \hat{c} \exp(-\alpha^2 t^*)$:

$$c^*(x^*, t^*) = \sum_{n=1}^{\infty} 2\lambda_n \sin(\lambda_n x^*) \left\{ \frac{1 - \exp[-t^*(\alpha^2 + \lambda_n^2)]}{(\alpha^2 + \lambda_n^2)} \right\}. \quad (54)$$

with $\lambda_n = (n - 1/2)\pi + \alpha^2$, $n \in \mathbb{Z}^+$ and time profile as follow:

$$c^*(t^*) = \sum_{n=1}^{\infty} 2[1 - \cos(\lambda_n)] \left\{ \frac{1 - \exp[-t^*(\alpha^2 + \lambda_n^2)]}{(\alpha^2 + \lambda_n^2)} \right\}. \quad (55)$$

Figures 7 and 8 show (54) and (55) for $\alpha^2 = 0.01$ and $\alpha^2 = 1$ for different times.

VI. Solutions to the recovery process

We will calculate the recovery process for three cases: no adsorption from separation of variables, adsorption with zero-flux and with non-zero flux at the end of the pores. Notice that for the similarity solution, the steady-state is never reached.

VI.1. Recovery step without adsorption

The solution of the diffusion problem without adsorption is given by Eq. (36), where the steady-state is reached at $c^*(x^*, \infty) = 1$.

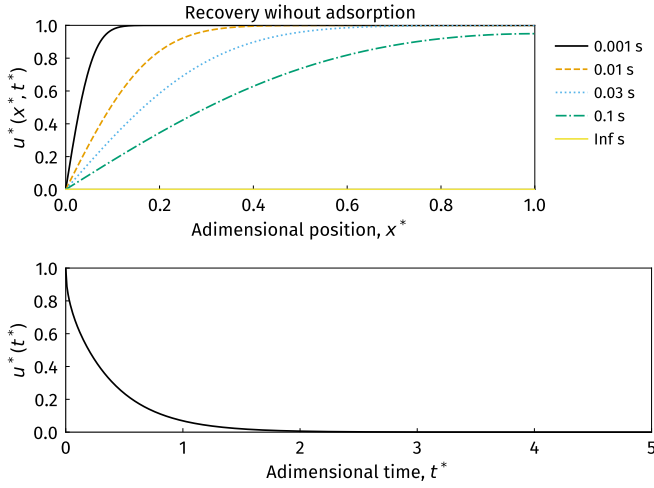


Fig. 9: Concentration profiles in the recovery process without adsorption: (top) Eq. (57) with legends indicating different t^* ; (bottom) Eq. (58).

Then, the problem to solve is as follow:

$$(DE): \quad \partial_t u^* = \partial_{xx} u^*, \quad (56a)$$

$$(BC-1): \quad u^*(0, t^*) = 0, \quad (56b)$$

$$(BC-2): \quad \partial_x u^*(1, t^*) = 0, \quad (56c)$$

$$(IC): \quad u^*(x^*, 0) = 1. \quad (56d)$$

The solution of this problem is similar to that of (21), except for the negative sign in the IC. Following the same procedure, we calculated the solution by separation of variables to be

$$u^*(x^*, t^*) = \sum_{n=1}^{\infty} \frac{2}{\lambda_n} \sin(\lambda_n x^*) \exp(-\lambda_n^2 t^*). \quad (57)$$

with $\lambda_n = (n - 1/2)\pi$, $n \in \mathbb{Z}^+$ and time profile

$$u^*(t^*) = \sum_{n=1}^{\infty} \frac{2}{\lambda_n^2} \exp(-\lambda_n^2 t^*). \quad (58)$$

Figure 9 shows the recovery solutions for non-adsorption.

VI.2. Recovery step with surface adsorption

The solution of the diffusion problem is given by Eq. (41) and the recovery process by

$$(DE): \quad \partial_t u^* = \partial_{xx} u^* - \alpha^2 u^*, \quad (59a)$$

$$(BC-1): \quad u^*(0, t^*) = 0, \quad (59b)$$

$$(BC-2): \quad \partial_x u^*(1, t^*) = 0, \quad (59c)$$

$$(IC): \quad u^*(x^*, 0) = 1 - \sum_{n=1}^{\infty} \left(\frac{2}{\lambda_n} \right) \left(\frac{\alpha^2}{\alpha^2 + \lambda_n^2} \right) \sin(\lambda_n x^*). \quad (59d)$$

We solve the homogeneous DE using Danckwerts' method, the

problem becomes

$$(DE): \quad \partial_t \hat{u} = \partial_{xx} \hat{u}, \quad (60a)$$

$$(BC-1): \quad \hat{u}(0, t^*) = 0, \quad (60b)$$

$$(BC-2): \quad \partial_x \hat{u}(1, t^*) = 0, \quad (60c)$$

$$(IC): \quad \hat{u}(x^*, 0) = 1 - \sum_{n=1}^{\infty} \left(\frac{2}{\lambda_n} \right) \left(\frac{\alpha^2}{\alpha^2 + \lambda_n^2} \right) \sin(\lambda_n x^*). \quad (60d)$$

Separation of variables, $\hat{u}(x^*, t^*) = p(x^*)q(t^*)$, leads to the boundary value problem

$$(DE): \quad p'' + \lambda p = 0, \quad (61a)$$

$$(BC-1): \quad p(0) = 0, \quad (61b)$$

$$(BC-2): \quad p'(1) = 0, \quad (61c)$$

with same solution as that of (23) with $p(x^*) = A_2 \sin(\lambda_n x^*)$ and $\lambda_n = (n - 1/2)\pi$, $n \in \mathbb{Z}^+$. Setting $q(t^*) = q(0) \exp(-\lambda_n^2 t^*)$, we get

$$\hat{u}^*(x^*, t^*) = \sum_{n=1}^{\infty} B_n \sin(\lambda_n x^*) \exp(-\lambda_n^2 t^*). \quad (62)$$

where $B_n = A_2 q(0)$. Applying the IC we calculate B_n as follow:

$$\begin{aligned} \hat{u}^*(x^*, 0) &= \sum_{n=1}^{\infty} B_n \sin(\lambda_n x^*) \\ \int_0^1 \hat{u}^*(x^*, 0) \sin(\lambda_m x^*) dx^* &= \int_0^1 \sum_{n=1}^{\infty} B_n \sin(\lambda_n x^*) dx^*. \end{aligned} \quad (63)$$

Replacing $\hat{u}^*(x^*, 0)$ by IC (60d) and using the orthogonality property of sines in Eq. (63), we find

$$B_n = \frac{2\lambda_n}{\alpha^2 + \lambda_n^2}. \quad (64)$$

Then,

$$\hat{u}^*(x^*, t^*) = \sum_{n=1}^{\infty} 2 \left(\frac{2\lambda_n}{\alpha^2 + \lambda_n^2} \right) \sin(\lambda_n x^*) \exp(-\lambda_n^2 t^*). \quad (65)$$

Combining last expression with (40), we find

$$u^*(x^*, t^*) = \sum_{n=1}^{\infty} 2 \sin(\lambda_n x^*) \left\{ \frac{\lambda_n [\alpha^2 + \lambda_n^2 \exp[-t^*(\alpha^2 + \lambda_n^2)]]}{(\alpha^2 + \lambda_n^2)^2} \right\}. \quad (66)$$

with $\lambda_n = (n - 1/2)\pi$, $n \in \mathbb{Z}^+$. The time profile is given by

$$u^*(x^*) = \sum_{n=1}^{\infty} 2 \left\{ \frac{[\alpha^2 + \lambda_n^2 \exp[-t^*(\alpha^2 + \lambda_n^2)]]}{(\alpha^2 + \lambda_n^2)^2} \right\}. \quad (67)$$

Figures 10 and 11 show the recovery solutions considering surface adsorption with zero flux at the end of the pores for two values of α .

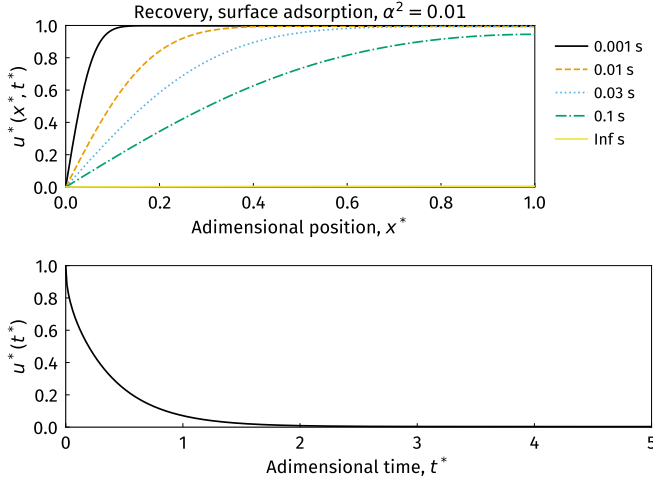


Fig. 10: Concentration profiles using the separation of variables solution: (top) Eq. (66) with legends indicating different t^* ; (bottom) Eq. (67). For all cases, $\alpha^2 = 0.01$.

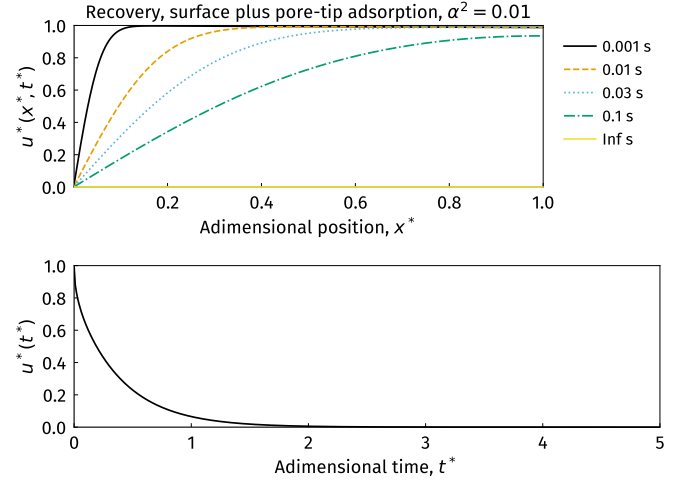


Fig. 12: Concentration profiles using the separation of variables solution: (top) Eq. (73) with legends indicating different t^* ; (bottom) Eq. (74). For all cases, $\alpha^2 = 0.01$.

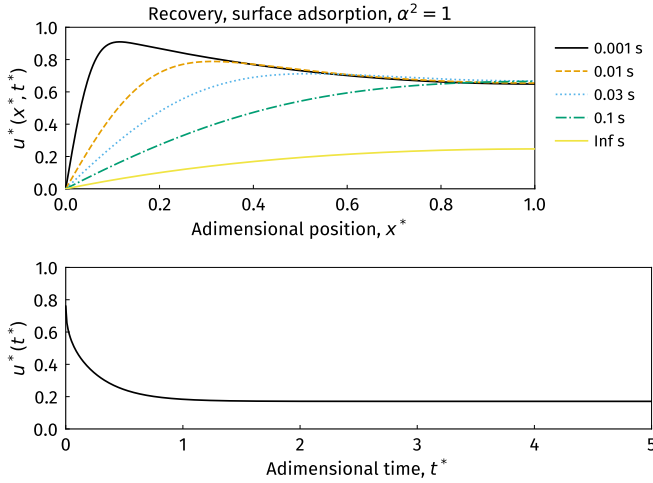


Fig. 11: Concentration profiles using the separation of variables solution: (top) Eq. (66) with legends indicating different t^* ; (bottom) Eq. (67). For all cases, $\alpha^2 = 1$.

VI.3. Recovery step with surface and pore-end adsorption

The problem is defined as follow:

$$(DE): \quad \partial_t u^* = \partial_{xx} u^* - \alpha^2 u^*, \quad (68a)$$

$$(BC-1): \quad u^*(0, t^*) = 0, \quad (68b)$$

$$(BC-2): \quad \partial_x u^*(1, t^*) + \alpha^2 u^*(1, t^*) = 0, \quad (68c)$$

$$(IC): \quad u^*(x^*, 0) = \sum_{n=1}^{\infty} \left(\frac{2\lambda_n}{\alpha^2 + \lambda_n^2} \right) \sin(\lambda_n x^*). \quad (68d)$$

where the IC is given by the steady-state of Eq. (54). Using the

transformation $u^* = \hat{u} \exp(-\alpha^2 t^*)$ we have

$$(DE): \quad \partial_t \hat{u} = \partial_{xx} \hat{u}, \quad (69a)$$

$$(BC-1): \quad \hat{u}(0, t^*) = 0, \quad (69b)$$

$$(BC-2): \quad \partial_x \hat{u}(1, t^*) + \alpha^2 \hat{u}(1, t^*) = 0, \quad (69c)$$

$$(IC): \quad \hat{u}(x^*, 0) = \sum_{n=1}^{\infty} \left(\frac{2\lambda_n}{\alpha^2 + \lambda_n^2} \right) \sin(\lambda_n x^*). \quad (69d)$$

Separation of variables leads to the following boundary value problem:

$$(DE): \quad p'' + \lambda p = 0, \quad (70a)$$

$$(BC-1): \quad p(0) = 0, \quad (70b)$$

$$(BC-2): \quad p'(1) + \alpha^2 p(1) = 0, \quad (70c)$$

Problem (70) is the same as (47), with $p_n(x^*) = \sin(\lambda_n x^*)$ and $\lambda_n = (n - 1/2)\pi + \alpha^2$, $n \in \mathbb{Z}^+$. We consider a time solution of the form $q(t^*) = q(0) \exp(-\lambda_n^2 t^*)$, with

$$q(0) = \frac{2\lambda_n}{\alpha^2 + \lambda_n^2} \quad (71)$$

calculated as above. Then, the solution to (69) is

$$\hat{u}(x^*, t^*) = \sum_{n=1}^{\infty} \left(\frac{2\lambda_n}{\alpha^2 + \lambda_n^2} \right) \sin(\lambda_n x^*) \exp(-\lambda_n^2 t^*). \quad (72)$$

Using the anti-transformation, $u^* = \hat{u} \exp(-\alpha^2 t^*)$, we arrive at the solution of (68):

$$u^*(x^*, t^*) = \sum_{n=1}^{\infty} \left(\frac{2\lambda_n}{\alpha^2 + \lambda_n^2} \right) \sin(\lambda_n x^*) \exp[-t^*(\alpha^2 + \lambda_n^2)] \quad (73)$$

with time profile

$$u^*(t^*) = \sum_{n=1}^{\infty} 2 \left[\frac{1 - \cos(\lambda_n)}{\alpha^2 + \lambda_n^2} \right] \exp[-t^*(\alpha^2 + \lambda_n^2)]. \quad (74)$$

Figures 12 and 13 show the recovery solutions considering surface adsorption with zero flux at the end of the pores for two values of α .

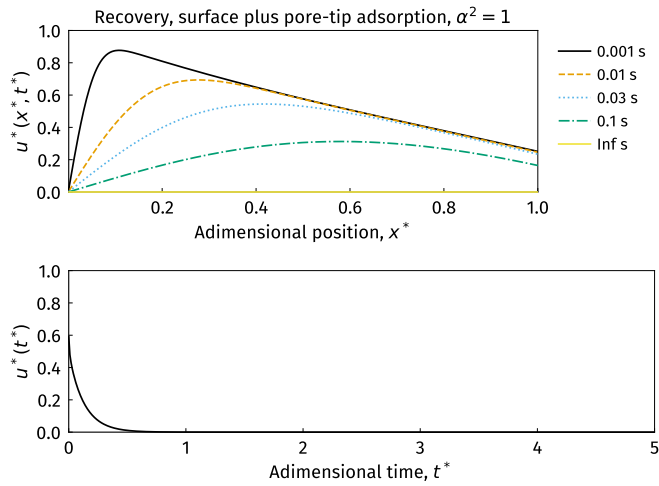


Fig. 13: Concentration profiles using the separation of variables solution: (top) Eq. (73) with legends indicating different t^* ; (bottom) Eq. (74). For all cases, $\alpha^2 = 1$.

- [1] O. Bisi, E. Ossicini, and L. Pavesi. Porous silicon: A quantum sponge structure for silicon based optoelectronics. *Surface Science Reports*, 38:1–126, 2000.
- [2] W. Theiß. Optical properties of porous silicon. *Surface Science Reports*, 29(3–4):91–192, 1997.
- [3] J. A. Monsour, R. A. Depine, and E. Silvestre. Porous silicon: A quantum sponge structure for silicon based optoelectronics. *Journal of the European Optical Society - Rapid Publications*, 2:07002, 2007.
- [4] H. Ouyang, M. Christophersen, R. Viard, B. L. Miller, and P. M. Fauchet. Macroporous silicon microcavities for macromolecule detection. *Advanced Functional Materials*, 15(11):1851–1859, 2005.

- [5] A. C. vanPohta, J. J. Steele, S. Tsoi, J. G. C. Veinot, M. J. Brett, and J. C. Sit. Porous nanostructured optical filters rendered insensitive to humidity by vapor-phase functionalization. *Advanced Functional Materials*, 16(10):1331–1336, 2006.
- [6] L. N. Acquaroli, R. Urteaga, and R. R. Koropecski. Innovative design for optical porous silicon gas sensor. *Sensors and Actuators B: Chemical*, 149(1):189 – 193, 2010.
- [7] G. Korotcenkov and B. K. Cho. Porous semiconductors: Advanced material for gas sensor applications. *Critical Reviews in Solid State and Materials Sciences*, 35(1):1–37, 2010.
- [8] S. M. Haidary, E. P. Córcoles, and N. K. Ali. Nanoporous silicon as drug delivery systems for cancer therapies. *Journal of Nanomaterials*, 2012(4):830503, 2012.
- [9] L. N. Acquaroli, T. Kuchel, and N. H. Voelcker. Towards implantable porous silicon biosensors. *RSC Adv.*, 4:34768–34773, 2014.
- [10] T. Tieu, M. Alba, R. Elnathan, A. Cifuentes-Rius, and N. H. Voelcker. Advances in porous silicon-based nanomaterials for diagnostic and therapeutic applications. *Adv. Therap.*, 2(1):1800095, 2019.
- [11] P. A. Kottke, A. G. Fedorov, and J. L. Gole. *Multiscale Mass Transport in Porous Silicon Gas Sensors*, pages 139–168. Springer New York, New York, NY, 2009.
- [12] J. Crank. *The mathematics of diffusion*. Oxford University Press, 2nd edition, 1975.
- [13] R. Haberman. *Applied partial differential equations with Fourier series and boundary value problems*. Pearson Education, Inc., 5th edition, 2012.
- [14] D. W. Hahn and M. N. Özisik. *Heat conduction*. John Wiley & Sons, Inc., 3rd edition, 2012.
- [15] N. Matsunaga, G. Sakai, K. Shimano, and N. Yamazoe. Formulation of gas diffusion dynamics for thin film semiconductor gas sensor based on simple reaction–diffusion equation. *Sensors and Actuators B: Chemical*, 96(1):226 – 233, 2003.
- [16] K. Selvaraj, S. Kumar, and R. Lakshmanan. Analytical expression for concentration and sensitivity of a thin film semiconductor gas sensor. *Ain Shams Engineering Journal*, 5(3):885 – 893, 2014.